
LCC Comparison of Existing Structure with an Effect of Water Front on Chloride Attack

Md. Shafiqul Islam^{*,1} and Toshiharu Kishi²

^{*1}Associate Professor, Department of Civil Engineering, Rajshahi University of Engineering & Technology, BANGLADESH

^{*2} Professor, Institute of Industrial Science, University of Tokyo, JAPAN

Abstract

A recent research came up with the conclusion that water penetration front is the key issue regarding surface quality which dramatically change the service life as well as life cycle cost of RC structure. In this study, chloride ion profile was measured using cores taken from real structures situated in Hokkaido and samples from Miyazaki Linear Experiment Line, Daidogawa and from a tunnel structure. The samples were put into 10% NaCl solution in the laboratory to get Cl⁻ profile. Using the concept of inclusion of water front in the estimation of chloride profile, the samples from the inspected structures were analyzed. Based on this analysis durability design and LCC comparison among the structures are presented.

Keywords: surface quality; liquid water front; LCC; Inspection; Chloride.

1. Introduction

It is very difficult to predict the actual performance scenario of real in-situ structure without the inspection being done. In this context the structure situated in Hokkaido was inspected and the cores were brought to the laboratory to get actual profile of chloride ingress. In spite of difference in construction year chloride tends to stop at some certain depths. This behavior is similar to the work done by Takahashi Yuya [1] with the conclusion that water penetration depth is the governing position beyond which chloride does not move. Laboratory experiments were done for slag concrete, as of Hokkaido real structure, to know the absorption capacity and liquid water front.

Two different quality of concrete taken from Miyazaki Linear Experiment Line were put in 10% of NaCl solution in the laboratory and the profile confirms the difference between surface quality between them. Out of these two, good concrete shows the Cl⁻ stopping position clearly whereas bad one does not. Same situation happened comparing samples taken from Daidogawa and from a tunnel. A concept is developed to utilize this penetration front as surface quality parameter to get life cycle cost of structure.

^c Corresponding Author: Md. Shafiqul Islam

Email: islam94001@yahoo.com

© 2009-2015 All rights reserved. ISSR Journals

2. Background

Chloride profile of the cores taken from OKINAWA and their immersion test results clearly stated that liquid water front stops the chloride ion penetration as shown in **Fig. 1a and 1b** [1]. Three types of concrete namely B0, F1 and F2 that stands for Ordinary Portland Cement concrete, fly ash 1 and fly ash 2 concretes were used. Horizontal close indicates thicker wall with high humidity inside and vertical open indicates thin wall where low humidity inside.

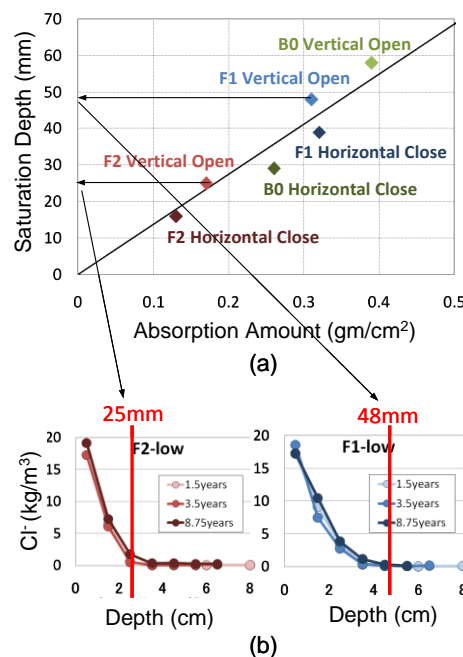


Figure 1. Comparison between Immersion test and Real Profile

The chloride stopping criterion due to liquid water front (w_f) will change the service life of the structure as explained in **Fig. 2**. In this figure liquid water front varies from 2 to 10 cm and the concentration of chloride is computed for depth of 6 cm. We can see a large difference in service life that will affect the life cycle cost also for the concrete having different surface quality in respect of liquid water front. The purpose of this study thus motivated to make a concept that helps to include liquid water front in LCC measurement.

The field engineers suppose that LCC will reduce due to having more durable materials in construction or by improvement of technology where the desk researchers at the design stage consider only Fick's law to predict chloride profile and that always overestimates the LCC. To reduce this gap between the images of LCC of two different professionals' inclusion of liquid water front in measurement of chloride profile is important.

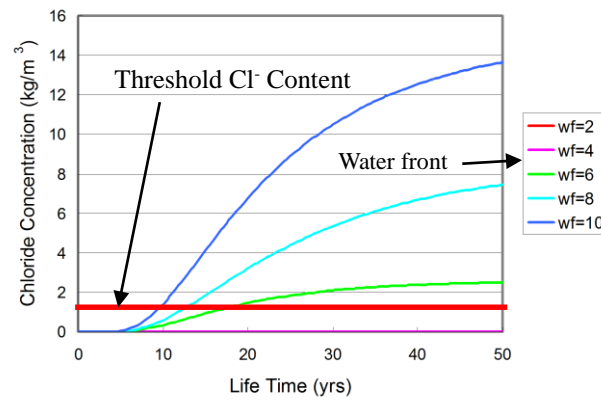


Figure 2. Effect of liquid water front on service life

3. Concept

The conceptual framework to use liquid water front in LCC is described briefly under sections 3.1, 3.2 and 3.3 stepwise.

3.1. Model modification

Chloride diffusion into concrete, like any diffusion process, is controlled by Fick's Second Law for non-steady state diffusion.

$$\frac{\partial C}{\partial t} = D \frac{\partial^2 C}{\partial x^2} \quad (1)$$

This includes the effect of changing concentration with time (t). This has been solved using the boundary condition $C_{(x=0, t>0)} = C_0$ (the surface concentration is constant at C_0), the initial condition $C_{(x>0, t=0)} = 0$ (the initial concentration in the concrete is 0) and the infinite point condition $C_{(x=\alpha, t>0)} = 0$ (far enough away from the surface, the concentration will always be 0). The solution is,

$$\frac{C(x, t)}{C_0} = 1 - \operatorname{erf}\left(\frac{x}{2\sqrt{Dt}}\right) \quad (2)$$

where $\operatorname{erf}(y)$ is the error function, a mathematical constant found in math tables or as a function in common computer spreadsheets, x is the cover depth, and $C(x, t)$ is the chloride concentration at time t and at depth x from the surface.

However, in actual practice, the flow is governed by the diffusion and convection manner [2, 3], and thus we have to use the following equation.

$$\frac{\partial C}{\partial t} = D \frac{\partial^2 C}{\partial x^2} - V \frac{\partial C}{\partial x} \quad (3)$$

Ogata and Banks [4] derived the solution for the above equation considering a semi-infinite column of porous media as follows.

$$\frac{C(x,t)}{C_0} = 0.5 \left[\operatorname{erfc} \frac{x-Vt}{2\sqrt{Dt}} + \exp\left(\frac{Vx}{D}\right) \operatorname{erfc} \left(\frac{x+Vt}{2\sqrt{Dt}}\right) \right] \quad (4)$$

where V is the average linear rate of flow (cm/s).

$$V = \frac{k}{\phi} \frac{\partial h}{\partial x} \quad (5)$$

where $\frac{\partial h}{\partial x}$ is the hydraulic gradient, which is considered constant as 0.1 MPa/m in this study, k is the hydraulic permeability (m/s), and ϕ is the porosity of the material. Porosity is dependent on other properties as the following equation, Eq. 6. The key parameters in this study are *diffusion coefficient* and *liquid water front*. In Eq. 5, the rate of flow is the function of hydraulic permeability (k) and porosity (ϕ), and these are dependent on the *diffusion coefficient* and *liquid water front*. Thus to determine the effects of the parameters only, the hydraulic gradient is kept constant.

$$\phi = \frac{1000 \times M}{\omega_f} \quad (6)$$

where M is the absorption capacity (gm/mm²) and w_f is the liquid water front (cm). Hydraulic permeability and the critical pore radius are determined by the experimental results as shown in **Fig. 3** stated in the references [5].

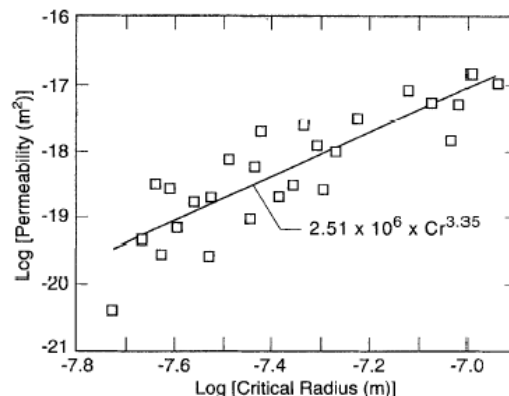


Figure 3. Permeability vs. critical pore radius

The critical pore radius, which is designated as r in this study, can be determined by capillary theory according to the following equation.

$$r(m) = \sqrt{\frac{4\mu}{P_o}} \times \frac{\omega_f}{\sqrt{t}} \quad (7)$$

where t is the time for short term absorption in seconds, w_f is the water front in cm, μ is the viscosity in pa-s, and P_o is atmospheric pressure in pa.

In Eq. 3, the diffusion coefficient is found from experiments done in the laboratory and the solution is based on the Finite Difference Method that will be discussed in the next section.

The surface chloride concentration C_o is considered to increase with time and is calculated as follows [6].

$$C_o(t) = C_{ou} (1 - \exp^{-\alpha t}) \quad (8)$$

where α is an environmental factor adopted as 0.50, t is time in years, and C_{ou} is the ultimate surface chloride.

Diffusion coefficient D is assumed to obey the following rule to make compatible with the stopping criterion of chloride ion up to the liquid water front. In **Fig. 4**, MFD, MFP and F stand for Modified Fick Deterministic, Modified Fick Probabilistic and Fick respectively.

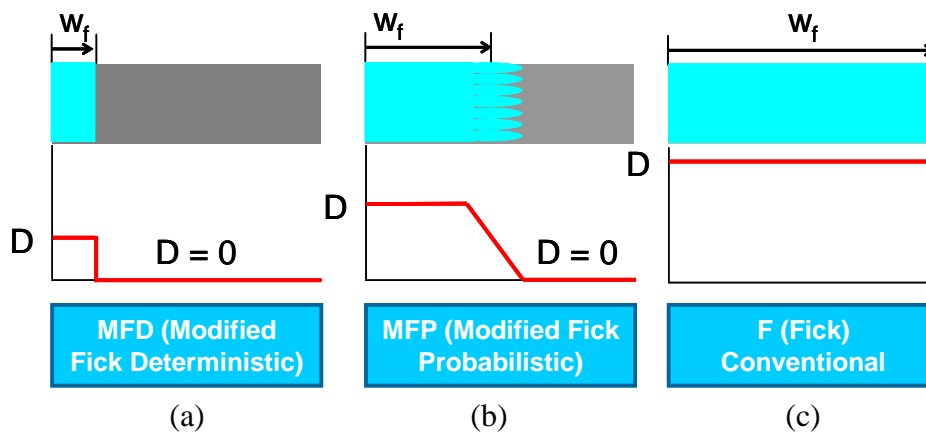


Figure 4. Coupling between liquid water front and diffusion coefficient

Fig. 4c shows the conventional way of thinking, which does not take into account the liquid water front, whereas the Modified Fick Deterministic and Modified Fick Probabilistic ways of thinking include the influence of the liquid water front on the chloride stopping criterion, diffusion coefficient D , which is set to the value shown in **Fig. 4a and 4b**. Under the conventional Fick's law, the diffusion coefficient is set as a constant throughout the specimen depth, whereas in the case of the modified Fick models, the diffusion coefficient is set differently in step with the liquid water front. In the case of bad quality concrete, saturation drops in the deeper zone from the surface where the diffusion coefficient drops slightly, but for the ease of calculation, it is assumed to be constant

throughout the specimen depth, based on the premise that the specimen is saturated almost in its entirety. In the case of large pores, Cl^- can move through the unsaturated zone inside. In the case of good quality concrete, saturation drops with the sharpness of the water front, and thus two values are needed for the diffusion coefficient, as shown in **Fig. 4a**. The medium quality type of concrete has both large and small pores, which makes the water front penetrate in a distribution pattern where the diffusion coefficient should be considered to decline along a slope until it reaches zero.

Matric pressure or capillary pressure is thought of as the pressure of water in a pore of the medium relative to the pressure of the air. If the matric pressure is close to zero, air-water interfaces are broadly curved, nearly all pores are filled and water content is high. If matric pressure is much less than zero the interfaces are more tightly curved, they can no longer go across the largest pore, and the pores have less water inside. Actually the curvature of the air-water interface is inversely related to the pressure. Tighter curvature is associated with smaller pores with more negative pressure. That is why in bad quality concrete having many larger pores, the water front variation is large and Cl^- can move through unsaturated parts with less wall friction. However, in good quality concrete, it is difficult to achieve the fully saturated condition and the pores inside remain disconnected. Moreover, good cover concrete having fine pores, a sharp front of water is expected, and if water can move through the even finer pores, Cl^- flow will be restricted by the wall friction.

3.2. Reliability based failure

The structural performance function of state ‘z’ for corrosion initiation of reinforcing steel and crack width are shown below.

$$z = C_{\text{lim}} - C(x, t) \quad (9)$$

$$z = w_d - w_c \quad (10)$$

Equations 9 and 10 can be generalized as load –capacity model as shown in Eq. 11.

$$\text{Performance} = \text{Strength} - \text{Load} = A - B \quad (11)$$

where ‘ C_{lim} ’ and w_d are the threshold chloride concentration and maximum allowable crack width, ‘ $C(x, t)$ ’ is chloride ion concentration (kg/m^3) and is solved using Eq. 3 by finite difference method, ‘ w_c ’ is the crack width (mm) as reference [7].

Reliability index can be determined using load-capacity model.

$$\beta = \frac{1}{V_z} = \frac{\mu_z}{\sigma_z} = \frac{\mu_{\ln A} - \mu_{\ln B}}{\sqrt{\sigma_{\ln A}^2 + \sigma_{\ln B}^2}} \quad (12)$$

‘ V_z ’ is the coefficient of variation of performance function ‘z’. All random variables are taken as log-normal distribution. Thus ‘ $\mu_{\ln A}$ ’, ‘ $\mu_{\ln B}$ ’, ‘ $\sigma_{\ln A}$ ’ and ‘ $\sigma_{\ln B}$ ’ are the mean of strength, load and standard deviation of strength, load respectively.

$$P_f(t) = \phi(-\beta) \quad (13)$$

The deteriorating structure is characterized by probability of failure ‘ $P_f(t)$ ’ or damage over the

interval $[0, T]$ as shown in Eq. 13 where ' φ ' is the standard normal cumulative distribution function. The reliability or performance index of structure thus comes to as follow.

$$R(t) = 1 - P_f(t) \quad (14)$$

The time to initiation of corrosion is referred as ' t_i ' and ' t_{cr} ' is named as time to reach allowable crack. Thus, the study reports the failure time as the summation of both the times indicated above.

$$t_f = t_i + t_{cr} \quad (15)$$

It is assumed that when ' $R(t) < 0.8$ ' structure needs repair.

3.3. Life cycle cost estimation

Life cycle cost regarded as LCC plays key role in maintaining the infrastructure and provides necessary information to the manager or owner. The definition of LCC in this study is considered as stated in the following equation.

$$LCC = InitialCost + \sum_{t=0}^T (AgingCost + RepairCost) \quad (16)$$

The three terms in the right hand side were accounted as explained by the following sections.

3.3.1. Initial cost

Initial cost is incorporated in the way below.

$$InitialCost = (unitcost \times area) \times (1 + \alpha T_{lifetime}) \quad (17)$$

where ' α ' is the cost of durability and is determined by the ration of cover to liquid water front, ' $T_{lifetime}$ ' is the design lifetime of the structure.

3.3.2. Aging cost

This is the cost carried by the owner due to regular maintenance operation. Aging cost is assumed to be proportional to the failure probability, as both of them increase with the increase of age of the infrastructure.

$$Aging Cost = Initial Cost \times 0.05 \times P(f)_{t_i} \quad \dots \dots u = 0 \quad (18)$$

$$Aging Cost = Initial Cost \times 0.05 \times P(f)_{t-t} \quad \dots \dots u = 1 \quad (19)$$

It is assumed that 5% of initial construction cost will be expended for maintenance. ' $P(f)_t$ ' is the probability of failure at yrs. ' t ', number of repair is subscript ' i ', ' t_i ' is the i th repair, ' u ' is the decision for repair, $u=0$ means no repair and $u=1$ represents do repair.

3.3.3. Repair cost

This cost is provided by the owner due to repair when the performance goes down below the required. In this study the repair is taken to be happened at performance index of structure goes below 80% of initial. Repair cost is modeled as shown in **Fig. 5** below.

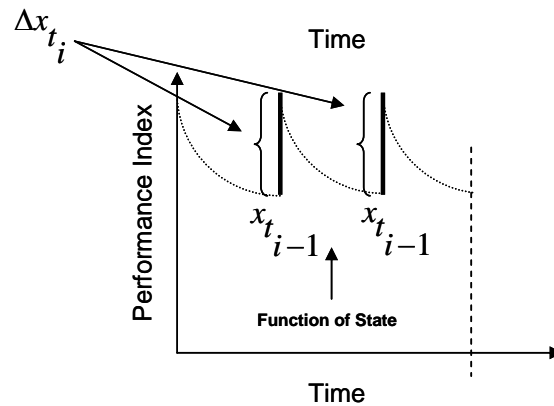


Figure 5. Concept of repairing cost

$$\text{Repair Cost} = 0 \quad \dots\dots u = 0 \quad (20)$$

$$\text{Repair Cost} = \left[\text{Fixed Cost} + \left(\text{unit Cost} \times \text{area} \times P(f)_{t_{i-1}} \times \Delta x_{t_i} \right) \right] \times \frac{{}^t_{RSL}}{{}^t_{\text{Repair}}} \quad (21)$$

$\dots\dots u = 1$

where *unit cost* is the cost of repair for unit area, ' $P(f)_{t_{i-1}}$ ' is the failure probability just before repair, ' Δx_{t_i} ' is the change of state done by repair 'i' at time 't', ' ${}^t_{RSL}$ ' is the residual service life in years, ' ${}^t_{\text{Repair}}$ ' is the life time of repair material.

It is assumed that the performance will be improved up to Δx_{t_i} that will meet initial level of performance. Cathodic protection is chosen as repair method with fixed and variable cost \$ 6870 and \$/m² 97 respectively [8].

4. Parameters from core data

Number of water retaining structures at Hokkaido was inspected to collect cores to analyze in the laboratory. All the structures were constructed with same slag concrete but in different years from 1994 to 1998. The cores were cut in 1 cm pitch and analyzed by titration according to JCI SC5 [9] and the profile is in Fig. 6.

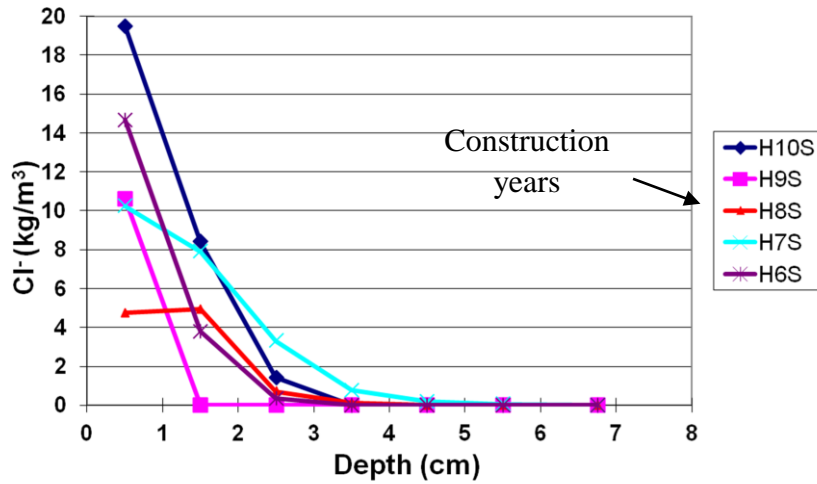


Figure 6. Chloride profile casted in different years (Hokkaido samples)

Samples collected from Miyazaki Linear Experiment Line, Daidogawa and from a tunnel structure were put in 10% NaCl solution in the laboratory and profiling was done in the same manner that of Hokkaido samples and are shown in **Fig. 7**, **Fig. 8**, **Fig. 9** and **Fig. 10**. The percentage of NaCl solution was fixed to 10% as it was a continuation of research work as of reference [1].

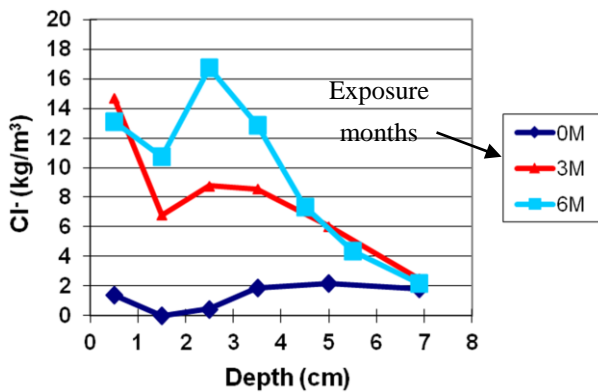


Figure 7. Chloride profile M083 (Miyazaki samples)

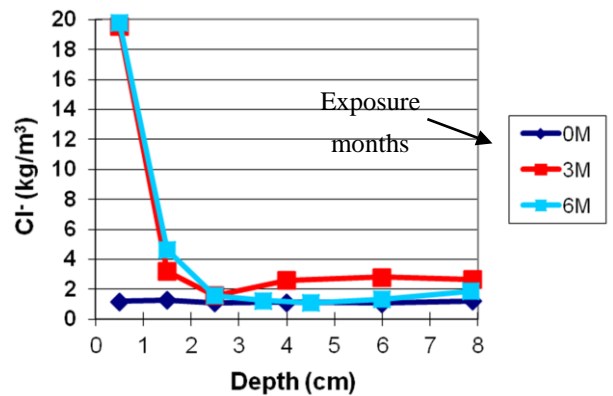


Figure 8. Chloride profile M112 (Miyazaki samples)

Fig. 6 shows stopping position around 4 cm for the case of Hokkaido samples. For Miyazaki Linear Experiment Line, intentionally 2 cases M083 and M112 are considered where we can see M083 has no stopping zone which represents bad surface quality and on the other hand M112 reflects stopping position at 3 cm and is treated as good concrete.

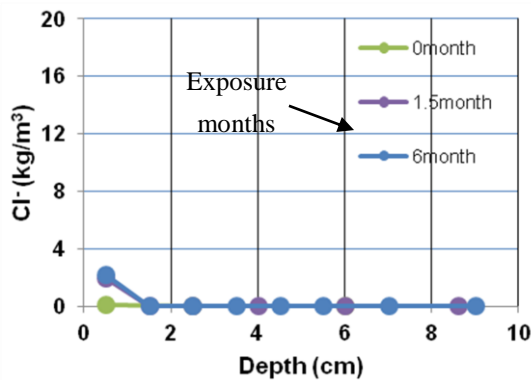


Figure 9. Chloride profile Daidogawa (Flange)

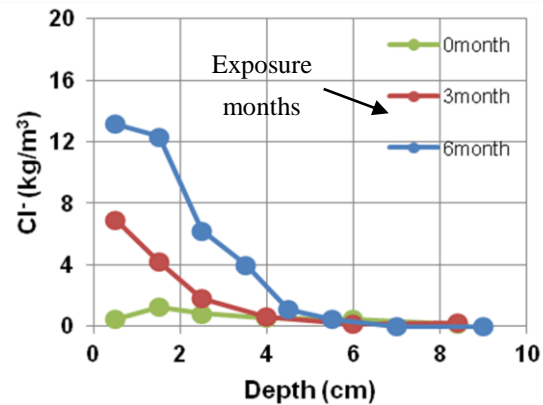


Figure 10. Chloride profile of a Train Tunnel

Another case of Daidogawa shows strong surface quality whereas the tunnel shows very bad in respect of penetration front. For the case of LCCA H7S and H10S are taken into account where Surface chloride C_o , diffusion coefficient D are different. Surface chloride C_o , diffusion coefficient D and liquid water front w_f are shown in **Table 1**.

TABLE 1: VARIABLE PARAMETERS

Name	C_o (kg/m ³)	D (cm ² /yr)	w_f (cm)
H7S	13.18	0.165	4
H10S	27.16	0.082	4
M083	16.04	1.650	10
M112	33.54	0.086	3
Daidogawa (Flange)	7.88	0.0847	2
Train Tunnel	15.96	2.653	6

5. Experimental study

Normal concrete and slag concrete with 50% replacement of cement by slag were cast in the laboratory. All the specimens were coated by primer and epoxy to make it non penetrable. The required surfaces were kept open. The specimens were put in 10% NaCl solution in three different exposure situations as horizontal, vertical open and vertical coated. Wet-dry cycles were maintained to simulate splash zone.

Wet condition was set as submergence in NaCl solution with temperature 20⁰C and 100% RH for 1 day and dry condition was set by keeping specimens inside 40⁰C chamber with 60% RH for 6 days. The weights for all the specimens were measured twice a week every after each condition. After the end of 3 months the specimens were broken and liquid water front were measured.

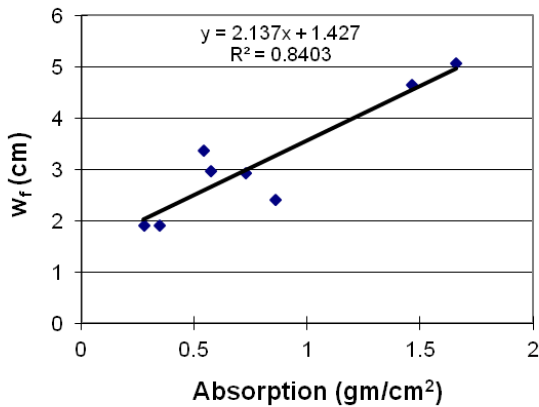


Figure 11. Correlation between absorption and liquid water front (Normal Concrete)

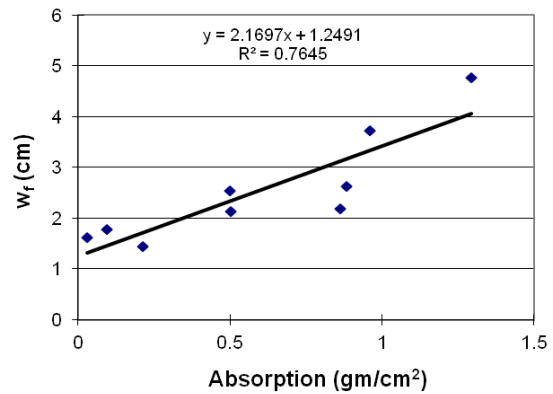


Figure 12. Correlation between absorption and liquid water front (Slag Concrete)

Absorption is determined from **Fig. 11** and **Fig. 12** for the penetration front stated in **Table 1** and will be used to compute service life and LCC of structure. Life cycle cost analysis was performed taking the parameters as log normally distributed with COV 0.1. Cover depth was kept fixed as 4 cm (mean) with COV 0.1.

6. Results and discussions

6.1. Effect of surface quality

The total cost normalized to initial cost (CT/CI) for H7S and H10S are same for 50 years of lifetime as shown in **Fig. 13**.

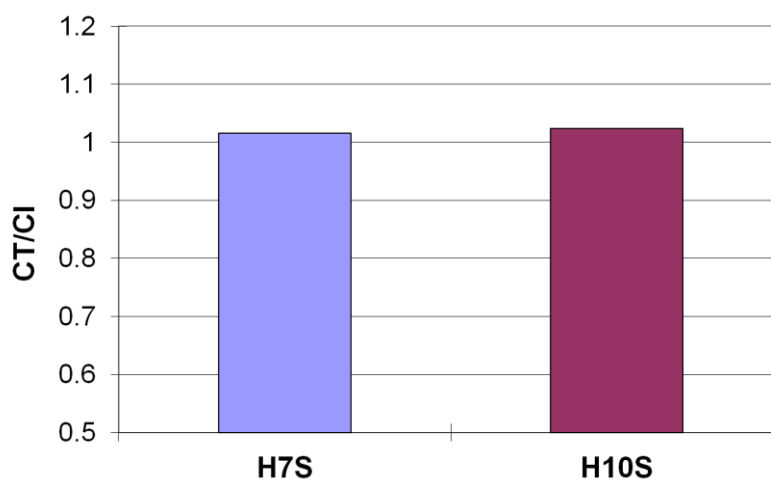


Figure 13. Comparison between Normalized Cost (H7S & H10S)

Although surface chloride and diffusion coefficient are different for the above two cases but liquid water front are almost the same as shown in **Fig. 6** that influenced the normalized costs to be

the same.

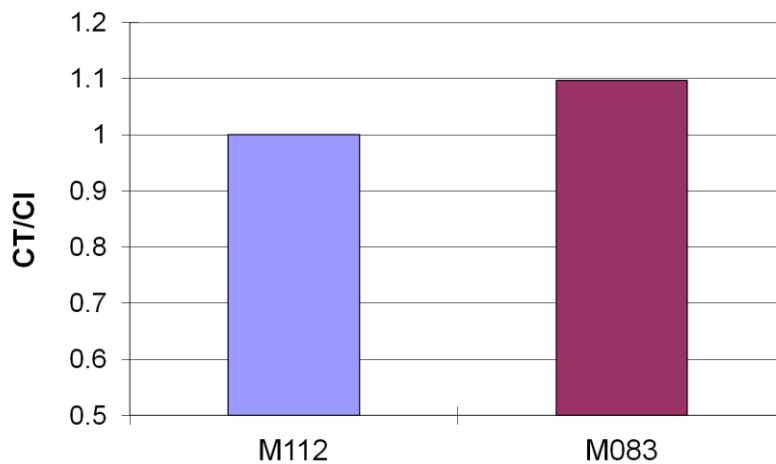


Figure 14. Comparison between Normalized Cost (M083 & M112)

On the other hand, M083 shows no stopping position of chloride shown in **Fig. 7** that reflects concrete with bad surface quality and with a definite small depth of stopping position of chloride for the case of M112 as shown in **Fig. 8** that reflects good quality of surface concrete. This variation of surface quality influence the total cost of M083 to be higher than that of M112 as shown in **Fig. 14** where 10% of additional cost is required to be expended throughout service life of the structure.

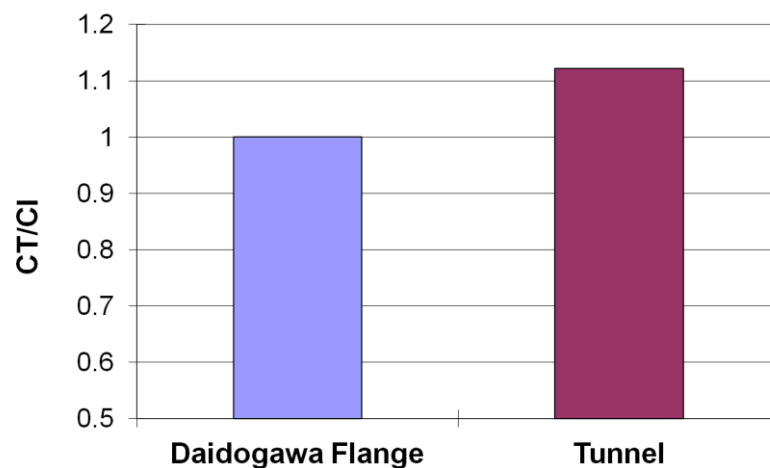


Figure 15. Comparison between Normalized Cost (Daidogawa & Tunnel)

Same explanation is suitable for Daidogawa and tunnel structure that shows the impact of penetration front on LCC that increase the total cost by 12% for bad concrete as shown in **Fig. 15**.

6.2. Impact of liquid water front on durability design

If the reinforcement location i.e. cover depth is sufficient enough that liquid water front cannot reach it, reinforcement will be safe against corrosion. Thus it is required to know how much cover depth is necessary to make the structure maintenance free. If total cost of the structure is normalized by initial cost and the value is unity is actually reflects that the structure is maintenance free.

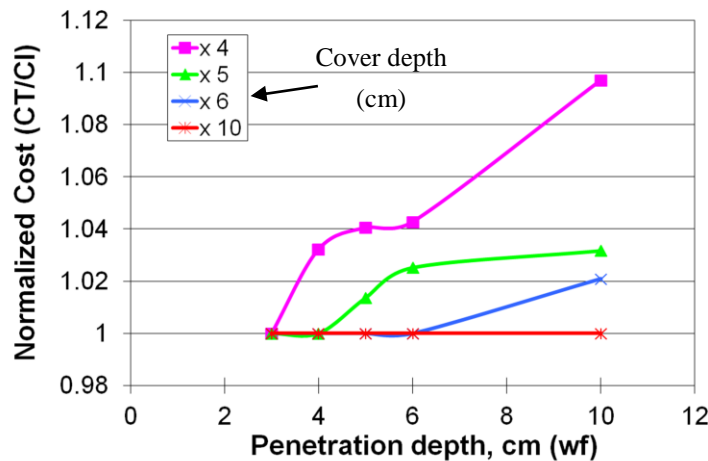


Figure 16. Impact of cover depth on normalized cost

Considering M112 case normalized cost is computed with varieties of cover depth from 4 to 10 cm and liquid water front from 3 to 10 cm. The increase the liquid water front increases the normalized cost and the increase in the cover depth decreases the normalized cost. Thus a boundary should exist to design cover depth to make the structure maintenance free, noted that, the life cycle analysis was performed considering 50 years of service life for all the cases.

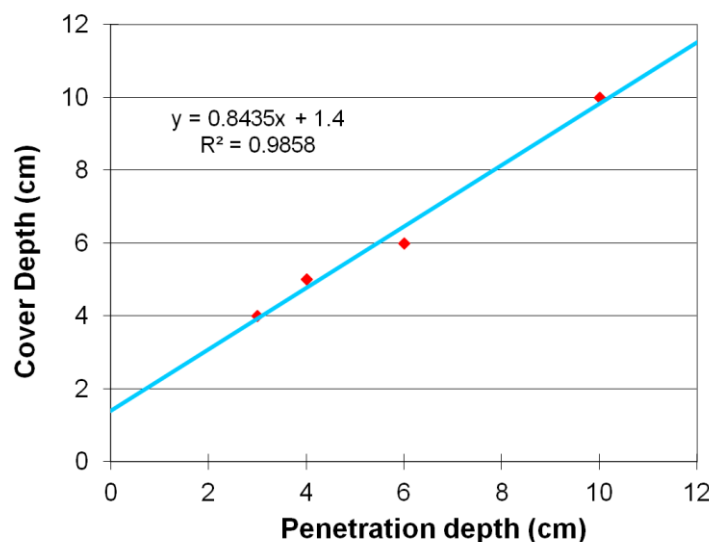


Figure 17. Cover design for liquid water depth

The straight line is the boundary that represents the safer and maintenance free structure against chloride attack for slag concrete. Cover depth should be maintained to some extent greater than liquid water depth to avoid maintenance. The top part, as shown in Fig. 17, is set as good concrete whereas

the bottom is bad that will be subjected to maintenance.

7. Conclusions

A concept is developed to take into account the liquid water front for service life and LCC prediction. By applying this concept to real structure, following remarks can be pointed out.

- (1) Surface quality is important parameter to take into account for LCCA.
- (2) Conventional way based on Fick's law will overestimate the LCC for concrete with good surface quality.
- (3) Good quality of concrete may not require LCCA if liquid water front is considered.
- (4) Geometry design of concrete should consider liquid water front as durability parameter.

References

- [1] Takahashi, Y. *Chloride ion Penetration Behavior in Concrete focused on Liquid Water Movement*. Master's thesis submitted to The University of Tokyo, 2010.
- [2] Bear, J. *Dynamics of Fluid in Porous Media*. Dover Publications, Inc. New York, 1988.
- [3] Freeze, R. A. and Cherry, J. A. *Groundwater*. Prentice-Hall, Inc. New Jersey, 1979.
- [4] Ogata, A., Banks, R.B. *A solution of the differential equation of longitudinal dispersion in porous media*. U.S. Geol. Surv. Prof. Papers 411-A, 1961.
- [5] Halamickova, P., Rachel, J., Detwiler, Bentz, D.P., Edward, J., Garboczi. *Water Permeability and Chloride Ion Diffusion in Portland Cement Mortars: Relationship to Sand Content and Critical Pore Diameter*. Cement and Concrete Research, 1995, **25**(4), p. 790-802.
- [6] Takeda, N., Sogo, S., Sakoda, S., Idemitsu, T. *An Experimental Study on Penetration of Chloride Ions into Concrete and Corrosion of Reinforcing Bars in Various Marine Environments*. Concrete Library of JSCE, 1999, **34**, p. 89-108.
- [7] Li, C. Q. *Life Cycle Modeling of Corrosion Affected Concrete Structures-Propagation*. Journal of Structural Engineering, 2003, ASCE, **129**(6), p. 753-761.
- [8] Strategic Highway Research Program. *National Research Council, "Cathodic Protection of Concrete Bridges. SHRP-S-372, USA, 1993-3.*
- [9] JCI SC5. *Abbreviated analysis method of all salinity which is included in the hardening concrete, Standard Method of Examination Regarding the Corrosion and Corrosion Protection of Concrete Structure*. Japan Concrete Institute, 1987.